

## EFFECT OF Cd<sup>2+</sup> IONS INSERTION ON STRUCTURAL, OPTICAL AND ELECTRICAL PROPERTIES OF Zn<sub>0.3</sub>Co<sub>0.7-x</sub>Cd<sub>x</sub>Fe<sub>2</sub>O<sub>4</sub> (0 ≤ x ≤ 0.7) FERRITES

N. AMIN<sup>a</sup>, M. I. ARSHAD<sup>a</sup>, M. AJAZ-UN-NABI<sup>a</sup>, K. MAHMOOD<sup>a</sup>,  
M. Z. IQBAL<sup>b</sup>, A. ALI<sup>a</sup>, M. T. WAHLA<sup>a</sup>, M. SHARIF<sup>a</sup>, M. ASIF<sup>c</sup>, N. SABAR<sup>a</sup>,  
S. IKRAM<sup>a</sup>, M. R. AHMAD<sup>d</sup>, Z. FAROOQ<sup>e</sup>, K. HUSSAIN<sup>a</sup>, A. BIBI<sup>f</sup>,  
G. MUSTAFA<sup>g\*</sup>

<sup>a</sup>Department of Physics, Government College University, Faisalabad 38000, Pakistan

<sup>b</sup>Department of Mathematics & Statistics, University of Agriculture Faisalabad

<sup>c</sup>Department of Physics, COMSATS University, Islamabad, Lahore Campus, 54500 Lahore, Pakistan

<sup>d</sup>Centre for Advanced Studies in Physics (CASp) G. C. University Lahore Pakistan

<sup>e</sup>Department of Physics, University of Education (Lahore) Faisalabad Campus, Faisalabad. 38000, Pakistan

<sup>f</sup>Laboratory of Nanoscale Biochemical Analysis, Jiangsu Key Laboratory for Carbon Based Functional Materials and Devices, Institute of Functional Nano and Soft Materials and Collaborative Innovation Centre of Suzhou Nanoscience and Technology, Soochow University, Suzhou, Jiangsu 215123, China

<sup>g</sup>Department of Physics, Bahauddin, Zakariya University Multan, 60800, Pakistan

The effect of cadmium ion insertion on structural, optical and electrical properties of Zn<sub>0.3</sub>Co<sub>0.7-x</sub>Cd<sub>x</sub>Fe<sub>2</sub>O<sub>4</sub> ferrites (0 ≤ x ≤ 0.7 with interval 0.14) have been characterized by XRD, EDX, FTIR, UV and I-V techniques. The material was synthesized using co-precipitation route. The growth of single phase cubic structure of samples was confirmed using XRD technique. The crystallite size was calculated from XRD spectra, which was found in the range of 27-39 nm. The FTIR spectra showed the two strong absorption bands at about 443 cm<sup>-1</sup> and 547.08 cm<sup>-1</sup> which confirmed their spinel cubic phase. The electrical resistivity of synthesized ferrites with the insertion of Cd<sup>2+</sup> ion was found to be in the range of 4.14 × 10<sup>8</sup> – 9.67 × 10<sup>8</sup> Ω-cm. The electrical resistivity was found to be decreasing with increase of temperature. The activation energy also increased with the increase of Cd<sup>2+</sup> and was found in the range of 0.02 - 0.05 eV.

(Received October 8, 2018; Accepted January 10, 2019)

**Keywords:** Spinel ferrites, Co-precipitation, XRD, Optical absorption, Dc-resistivity

### 1. Introduction

Soft ferrites play an important role in different fields of technological utilization that require high electrical resistivity at ambient temperatures and low electrical losses across a wide range of frequencies. Ferrites attained attention of researchers due to their comparatively low cost, high mechanical strength, chemical stability at high annealing temperatures and higher DC resistivity [1]. The ferrites have wonderful capability for tuning their magnetic properties [2]. There are various applications of soft ferrites in different areas such as satellite communication, computer components, memory devices, magnetic sensors, magnetic recording media, microwave absorbing materials, transformer cores, drug delivery and hyperthermia for cancer treatment, gas sensors and contrast improvement in magnetic resonance imaging [3-12]. It is reasonable to forecast the potential candidacy of spinel ferrite thin films as high density recoding media due to brilliant mechanical permanence and small noise quality [13-14]. Due to having remarkably low electrical conductivity and dielectric losses, ferrites nano particles are frequently used in the preparation of micro-wave devices [15-17]. To the best of our knowledge, there is an insufficient

\*Corresponding author: ghulammustafabzu@gmail.com

work in the literature on the Cd<sup>2+</sup> substituted Co-Zn ferrites. Narendra et al. reported that the Cd<sup>2+</sup>-substituted CoFe<sub>2</sub>O<sub>4</sub> nanoparticles exhibited the super paramagnetic behavior [18-21]. The properties of ferrites depend on synthesizing route, sintering temperature and different conditions applied. The distribution of cations between the tetrahedral and octahedral sites determines the structural, magnetic and electrical properties [22]. The present study focuses on structural, optical and electrical properties of Zn<sub>0.3</sub>Co<sub>0.7-x</sub>Cd<sub>x</sub>Fe<sub>2</sub>O<sub>4</sub> (0 ≤ x ≤ 0.7) ferrites synthesized by co-precipitation method.

## 2. Experimental detail

### 2.1. Sample preparation

Single phase spinel ferrites having general formula Zn<sub>0.3</sub>Co<sub>0.7-x</sub>Cd<sub>x</sub>Fe<sub>2</sub>O<sub>4</sub> (x = 0, 0.14, 0.28, 0.42, 0.56 and 0.7) were prepared by co-precipitation method with stoichiometric proportions of materials FeCl<sub>3</sub>.6H<sub>2</sub>O, ZnCl<sub>2</sub>, CdCl<sub>2</sub>.6H<sub>2</sub>O, and CoCl<sub>2</sub>.6H<sub>2</sub>O. The desired quantities of all chemicals were dissolved in deionized water separately. All the solutions were mixed on hot plate with magnetic stirrer at 50 °C and NaOH was added drop wise in mixture to maintain pH 12. The precipitates of the solutions were formed and placed in the preheated water bath at 90 °C for 2 h. The obtained precipitates were washed using deionized water twice and then placed in oven at 90 °C for 24 h for drying process. The precipitates were grinded to form fine powder of the samples. The powder was pressed into pellets using hydraulic press. Finally, the dried powder and pellets of all the samples were sintered at 900 °C for 2 h. The X-ray diffraction (XRD) patterns were recorded at room temperature using an Xpert Pro PANalytical diffractometer with Cu-Kα radiation (λ = 1.54056 Å) at 40 kV and 30 mA in the 2θ range of 20°-60°. The Fourier transform infrared spectra (FTIR) were recorded in the range 400 - 4000 cm<sup>-1</sup> using Jasco-310 spectrometer. The surface morphology of the samples was studied by JSM-6490 JEOL scanning electron microscope (SEM). The energy-dispersive X-ray (EDX) confirmed the elemental composition of the prepared samples. The energy band gap of the samples was determined by UV/Vis spectroscopy and current-voltage (I-V) characteristics were recorded by using two probe method.

### 2.2. Calculation

The recorded XRD patterns were used to calculate the structural parameters such as lattice constant, unit cell volume and crystallite size. The above mentioned parameters were calculated using the equations given below:

$$a = \frac{\lambda}{2\sin\theta} \sqrt{h^2 + k^2 + l^2} \quad (1)$$

$$V_{cell} = a^3 \quad (2)$$

$$D = \frac{k\lambda}{\beta_{hkl} \cos\theta} \quad (3)$$

Here (h k l) are the Miller indices, V<sub>cell</sub> is the unit cell volume, k is the shape factor, λ is the X-ray wavelength; θ is the Bragg's diffraction angle and β<sub>hkl</sub> represent full width at half maxima. For electrical measurements, the samples were pressed into disk shaped pellets. A silver paint was applied on both sides of the pellet to ensure good electric contact and the pellet was held between two electrodes of a specially designed sample holder.

## 3. Results and discussion

### 3.1. X-ray diffraction analysis

Fig. 1 shows the XRD patterns of Zn<sub>0.3</sub>Co<sub>0.7-x</sub>Cd<sub>x</sub>Fe<sub>2</sub>O<sub>4</sub> with x = 0, 0.14, 0.28, 0.42, 0.56 and 0.7. The XRD peaks corresponds to diffraction planes (220), (300), (311), (400), (422) and

(511) which confirm the formation of cubic spinel structure. All samples are single phase except that of  $x = 0.7$ . The peaks are indexed by using the computer software Jade5. By using the XRD data, following parameters have been calculated i.e. the lattice constant, unit cell volume and crystallite size using Eq. (1-3) respectively. The obtained values are listed in the Table 1. It is clear that lattice parameter of the pure sample at  $x = 0$  is  $8.3860 \text{ \AA}$  and at  $x = 0.7$  is  $8.6733 \text{ \AA}$  while the behavior of the lattice constant showing decreasing trend in the range ( $8.4610 \text{ \AA} - 8.3773 \text{ \AA}$ ). It was attributed that substitution of larger ionic radius (cadmium ions) for smaller ionic radius (cobalt) would normally increase the crystal size. In our case the behavior of cadmium at high sintering temperature became volatile due to deficiency of cadmium. The crystallite size of all the samples have been calculated using Scherer's formula which have been listed in Table 1, The crystallite size of the single phase sample ( $x = 0$ ) was  $27 \text{ nm}$  whereas it was  $39 \text{ nm}$  for  $x = 0.7$ . The increasing trend in the crystallite size from  $29 - 37.2 \text{ nm}$  was due to the increase in the content of cadmium. This increasing trend of crystallite size is shown in Fig. 2, and is attributed to the comparatively long sintering time that causes the reduction of  $\text{Fe}^{3+}$  ions to  $\text{Fe}^{2+}$  ions and results an increase in the lattice parameters. Therefore, the number of  $\text{F}^{2+}$  ions on the octahedral site plays a dominant role in increase of the crystal size [23-25].

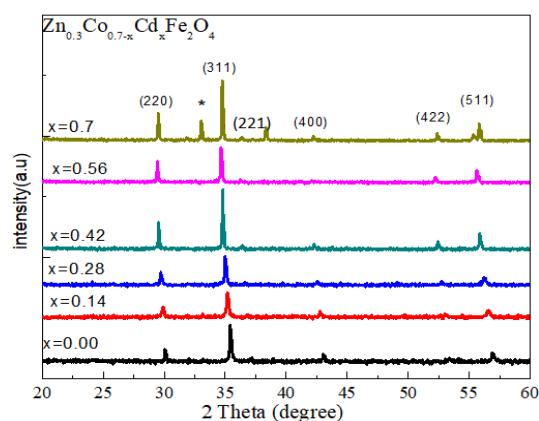


Fig. 1. XRD Patterns of  $\text{Zn}_{0.3}\text{Co}_{0.7-x}\text{Cd}_x\text{Fe}_2\text{O}_4$  ( $0 \leq x \leq 0.7$ ) ferrites.

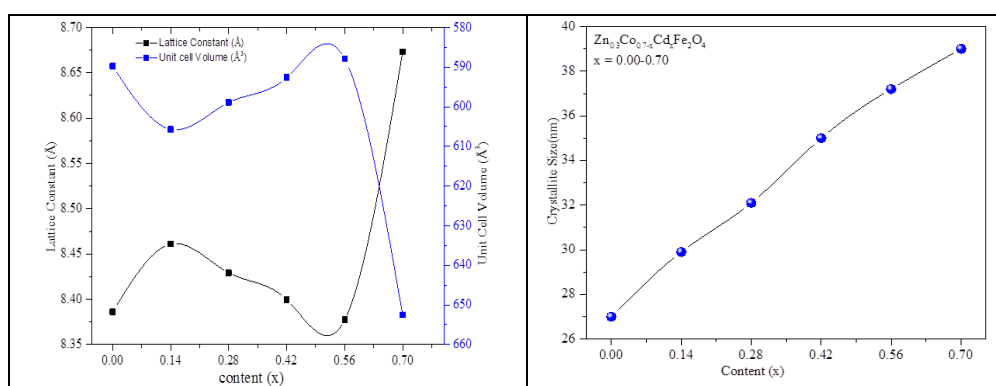


Fig. 2. (2a) Lattice Constant and unit cell volume versus content (x) (2b) Crystallite Size (nm) Versus Cd Content (x).

Table 1. Lattice constant, unit cell volume, crystallite size (nm), electrical resistivity ( $\Omega\text{-cm}$ ) and activation energy (eV) of  $\text{Zn}_{0.3}\text{Co}_{0.7-x}\text{Cd}_x\text{Fe}_2\text{O}_4$  ferrites

content (x)	Lattice constant ( $\text{\AA}$ )	Unit cell volume ( $\text{\AA}^3$ )	Crystallite Size (nm)	Resistivity ( $\Omega\text{-cm}$ ) $\times 10^8$	Activation Energy (eV)
0.00	8.3860	589.75	27	4.144	0.02
0.14	8.4610	605.71	29.9	4.794	0.015
0.28	8.4292	598.90	32.1	5.372	0.02
0.42	8.3996	592.62	35	7.426	0.03
0.56	8.3773	587.91	37.2	8.958	0.04
0.70	8.6733	562.47	39	9.676	0.05

### 3.2. Morphology and Elemental Analysis

The EDX technique is a powerful technique to determine the elemental composition of the materials. The elemental composition of the  $\text{Zn}_{0.3}\text{Co}_{0.7-x}\text{Cd}_x\text{Fe}_2\text{O}_4$  nanoparticles was studied using this technique. The obtained data presented in table 2 confirmed that the observed ratios of samples are close to the expected stoichiometry. The SEM images shown in Fig. 3 (a-c) verify the homogeneity among the samples [26].

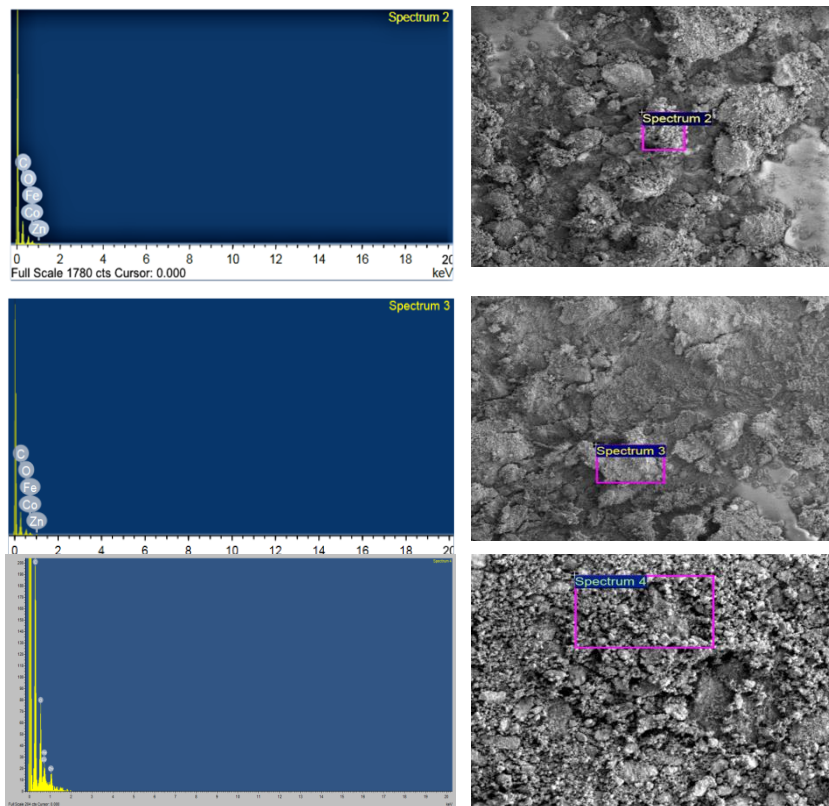


Fig. 3. EDX/SEM of  $\text{Zn}_{0.3}\text{Co}_{0.7-x}\text{Cd}_x\text{Fe}_2\text{O}_4$  ferrites (3a)  $x = 0.14$  (3b)  $x = 0.28$  and (3c)  $x = 0.42$ .

Table 2. The elemental analysis of  $\text{Zn}_{0.3}\text{Co}_{0.7-x}\text{Cd}_x\text{Fe}_2\text{O}_4$  nano ferrites.

Elements (%)	X=0.14	X= 0.42	X = 0.7
C	55.61	60.79	57.22
O	24.81	20.66	26.82
Fe	16.56	13.71	9.37
Cd	2.48	1.61	3.26
Co	1.93	3.06	0.35
Zn	1.72	2.39	2.56

### 3.3. FTIR analysis

The FTIR spectra of  $\text{Zn}_{0.3}\text{Co}_{0.7-x}\text{Cd}_x\text{Fe}_2\text{O}_4$  nano ferrites were recorded in the range of  $400\text{ cm}^{-1} - 4000\text{ cm}^{-1}$  as shown in Fig. 4. In general, the FTIR demonstrates two frequency bands in the range of  $400 - 1000\text{ cm}^{-1}$ , which are the characteristic bands of spinel ferrites. The absorption bands in the range of  $400 - 1000\text{ cm}^{-1}$  relates to the stretching and vibration of tetrahedral and octahedral sites. In our samples, the frequency bands are seen in the range of  $547\text{ cm}^{-1}$  and  $443\text{ cm}^{-1}$  which are associated to the stretching vibrations of tetrahedral and octahedral sites in all samples. The tetrahedral metal–oxygen band (Fe-O) of stretching vibration is related to high frequency absorption band, and in octahedral site it is associated to the low frequency band (Cd-O) [27].

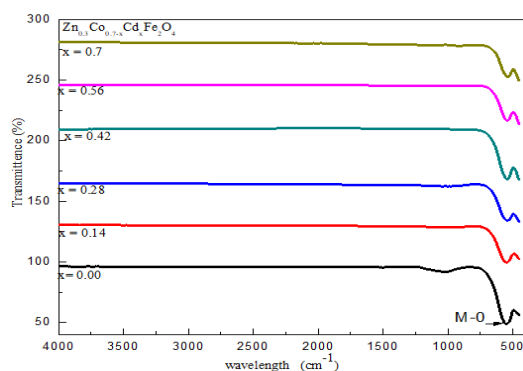


Fig. 4. FTIR spectra of  $\text{Zn}_{0.3}\text{Co}_{0.7-x}\text{Cd}_x\text{Fe}_2\text{O}_4$  ( $0 \leq x \leq 0.7$ ) ferrites.

### 3.4. Optical properties

Fig. 5 depicts the absorption (A%) variation for Cd substituted Co-Zn ferrites as the function of wavelength recorded in the wavelength range of 200 - 900 nm. The optical bandgap plays an important role to determine the applications of materials in optoelectronics.

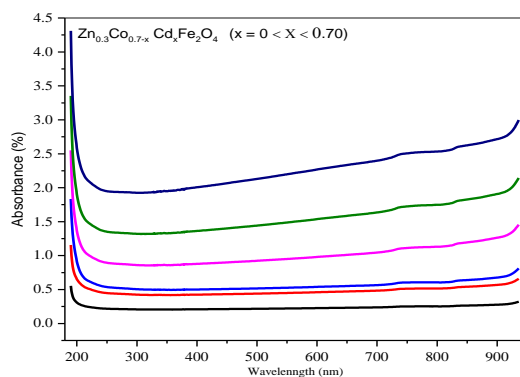


Fig. 5. Spectral absorbance of the Cd-substituted Co-Zn-ferrites ( $0.00 x \leq 0.7$ ).

The prominent sharpness in the peak was not observed in the UV-visible range from 390 nm to 790 nm which indicates that the colloidal have well dispersed [23]. The calculation of optical band gap for the representative sample is shown in the Fig. 6 and 7. The Tauc relation was used to calculate the optical band gap and is given below:

$$\alpha h\nu = A(h\nu - E_g)^n$$

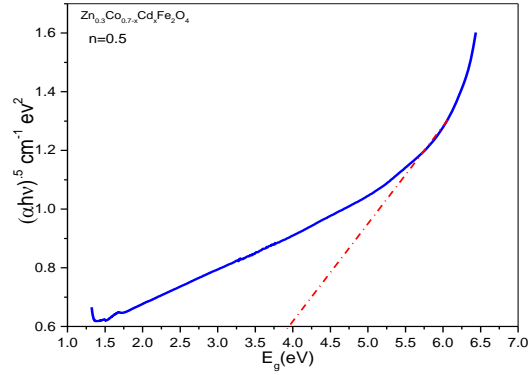


Fig. 6. Plot  $(\alpha h\nu)^2$  versus  $E_g$  (eV) at  $n = 0.5$ .

Here  $E_g$  is optical band gap,  $h\nu$  is energy of photons used,  $A$  is constant that depends on the transition probability,  $\alpha$  is absorption coefficient. The constant “ $n$ ” is dependent on material’s nature and exhibits value of 0.5 for direct bandgap materials and 2 for indirect bandgap materials [24-25].

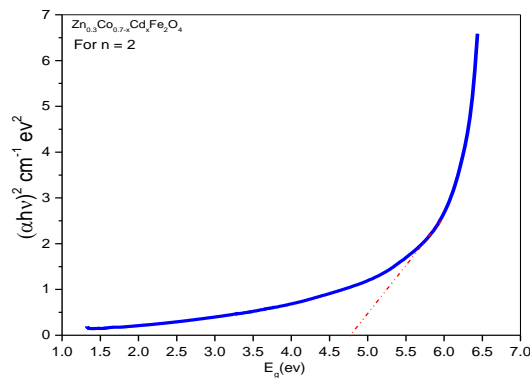


Fig. 7. Plot  $(\alpha h\nu)^{0.5}$  Versus  $E_g$ (ev) at  $n = 2$ .

### 3.5 Electrical properties

#### 3.5.1. Variation of dc resistivity versus temperature and composition

DC resistivity of each sample is calculated using the relation  $\rho = \frac{RA}{L}$  where “ $R$ ” is the resistance of the disk shaped samples,  $A$  is the cross-sectional area and  $L$  is the thickness of the sample [28].

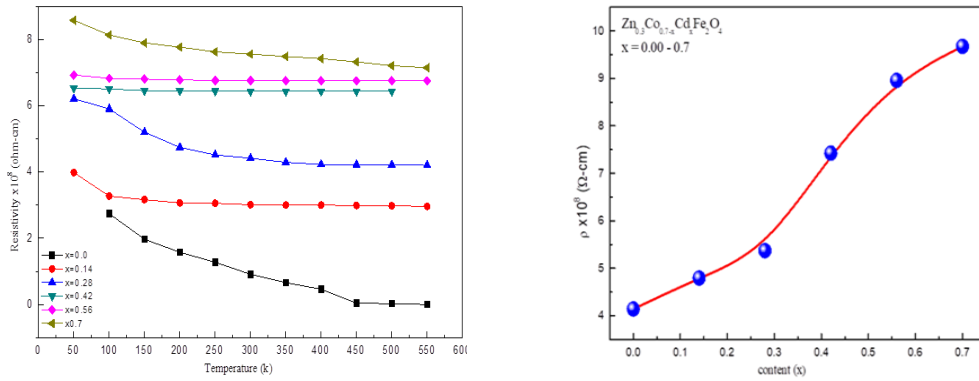


Fig. 8. Variation of Resistivity versus (8a) Temperature and (8b) Cd content (x).

Fig. 8 (a) & (b) illustrate the effect of electrical resistivity with temperature and Cd content, respectively. The value of electrical resistivity measured is found to be in the range of  $4.14 \times 10^8 - 9.67 \times 10^8 \Omega\text{-cm}$ . and shows a decreasing trend with increase in temperature. The observed results also revealed that electrical resistivity increases with the increase of Cd content. The similar results have been reported by Mamiya [29].

### 3.5.2. Variation of $\log(\rho)$ and activation energy versus temperature and Cd content (x)

Fig. 9 (a) illustrates the effect of electrical resistivity  $\log(\rho)$  Versus  $1000/T$ . These graphs were used to calculate the activation energy of charge carriers responsible for the conduction mechanism at higher temperatures in the Cd<sup>2+</sup> substituted Co-Zn ferrites using the relation [30]:

$$E_a = 0.198 * 10^{-3} \frac{d(\log \rho)}{d\left(\frac{1}{T}\right)}$$

where  $\rho$  is the resistivity,  $k_B$  is Boltzmann constant.

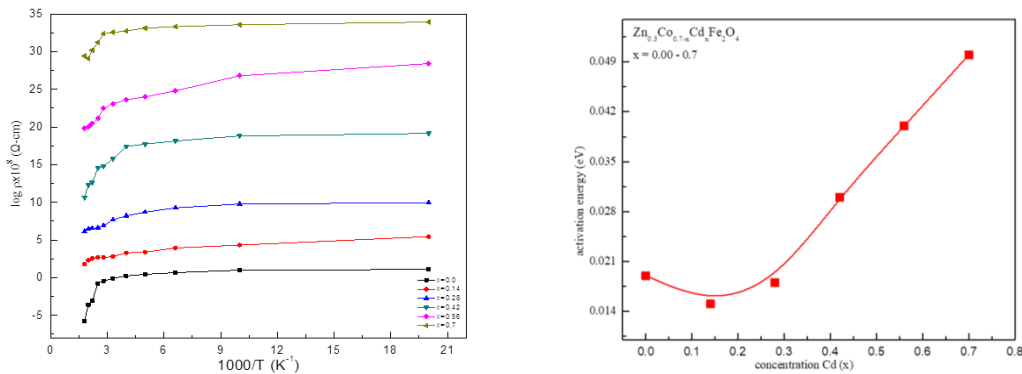


Fig. 9. (9a) Variation of  $\log(\rho)$  Versus  $1000/T$  (K<sup>-1</sup>) (9b) activation energy versus content (x).

The obtained values of activation energy were drawn as a function of Cd content in Fig. 9(b), which shows the increasing trend of activation energy with increasing Cd content. Rezlescu et al. reported that increase in the activation energy of charge carriers with increasing Cd content can be attributed to the substitution of cations at B sites [31]. Thus, the localization of Fe<sup>2+</sup> ions is responsible for the observed increase in the activation energy.

#### 4. Conclusions

A series of  $Zn_{0.3}Co_{0.7-x}Cd_xFe_2O_4$  where  $x = 0, 0.14, 0.28, 0.42, 0.56$  and  $0.7$ , spinel ferrites was synthesized using co-precipitation method. The successful growth of single phase spinel structure was evidenced by XRD analysis. The lattice constant of each sample was calculated and it was found in the range of  $8.386 - 8.470 \text{ \AA}$ . The crystallite size was found in the range of  $27 - 39 \text{ nm}$  which was measured using Scherer's formula. The compositional presence of Cd, Fe, Co, Zn and O elements in cadmium substituted zinc - cobalt ferrite was ensured by EDX spectra.

The FTIR spectra showed a good agreement with spinel cubic ferrites as two strong absorption bands were observed at  $443 \text{ cm}^{-1}$  and  $547.08 \text{ cm}^{-1}$ . The electrical resistivity of doped materials was recorded in the range of  $4.14 \times 10^8 - 9.67 \times 10^8 \text{ \Omega-cm}$ . The electrical resistivity of samples was decreased with increase of temperature. The activation energy of materials increased with increase of cadmium content which was found in the range of  $0.019 - 0.05 \text{ eV}$ . The results show that the optical, structural and electrical properties have been strongly effected with insertion of cadmium content due to which the material can be manipulated according to desired application.

#### Acknowledgements

The authors are thankful for providing characterization support to carry out this work under Govt. College University Faisalabad-RSP-Project # 159-PHY-5.

#### References

- [1] I. H. Gul, W. Ahmed, A. Maqsood, *J. Magn. Magn. Mater.* **320**, 270 (2008).
- [2] M. A. Gabal, Y. M. A. Angari, *Mater. Chem. Phys.* **118**, 153 (2009).
- [3] I. H. Gul, E. Pervaiz, *Mater. Res. Bull.* **46**, 1353 (2012).
- [4] Y. M. Abbas, S. A. Mansour, M. H. Ibrahim, S. E. Ali, *J. Magn. Magn. Mater.* **23**, 2748 (2011).
- [5] A. Thakur, P. Thakur, J. H. Hsu, *J. Appl. Phys.* **111**, 07A305 (2012).
- [6] S. Singhal, J. Singh, S. K. Barthwal, K. Chandra, *J. Solid State Chem.* **178**(10), 3183 (2005).
- [7] K. Muthuraman, S. Alagarsamy, M. A. Banu, V. Naidu, *Int. J. Comput. Appl.* **32**, (2011).
- [8] D. R. Mane, D. D. Birajdar, S. Patil, S. E. Shirsath, R. H. Kadam, *J. Sol-Gel Sci. Technol.* **58**, 70 (2010).
- [9] M. Hashim, K. S. Alimuddin, S. E. Shirsath, R. K. Kotnala, J. Shah, R. Kumar, *Mater. Chem. Phys.* **139**, 364 (2013).
- [10] K. M. Batoo, S. Kumar, *Int. J. Nanopart.* **2**, 416 (2009).
- [11] S. Kubickova, J. Vejpravova, P. Holec, D. Niznansky, *J. Magn. Magn. Mater.* **334**, 102 (2013).
- [12] P. P. Hankare, K. R. Sanadi, K. M. Garadkar, D. R. Patil, I. S. Mulla, *J. Alloy. Comp.* **553**, 383 (2013).
- [13] I. H. Gul, A. Maqsood, *J. Alloy. Comp.* **465**, 227 (2008).
- [14] B. H. Ryu, H. J. Chang, Y. M. Choi, K. J. Kong, J. O. Lee, C. G. Kim, H. K. Jung, J. H. Byun, *Phys. Stat. Sol. A* **201**, 1855 (2004).
- [15] N. Rezlescu, E. Rezlescu, C. Pasnicu, M. L. Craus, *J. Magn. Magn. Mater.* **136**, 319 (1994).
- [16] V. Sepelak, D. Baabe, F. J. Litterst, K. D. Becker; *J. Appl. Phys.* **88**, 5884 (2000).
- [17] Martha Pardavi-Horvath, *J. Magn. Magn. Mater.* **215**, 171 (2000).
- [18] A. M. M. Farea, Shalendra Kumar, Khalid Mijasam Batoo, Ali Yousef, Alimuddin, *Physica B* **403**, 684 (2008).
- [19] A. M. M. Farea, Shalendra Kumar, Khalid Mijasam Batoo, Ali Yousef, Chan Gyu Lee, *J. Alloy Compd.* **464**, 361 (2008).
- [20] R. Nongjai, Shakeel Khan, K. Asokan, Hilal Ahmed, Imran Khan, *J. Appl. Phys.* **112**, 084321 (2012).



- [21] B. Narendra, D. Bhaskar, G. Srinivas, R. V. S. S. N. Ravikumar, Ch. Venkata Reddy, IEEE (Proceedings) (2013) 181-183.
- [22] I. Ahmad, T. Abbas, M. U. Islam, A. Maqsood, Ceram. Int. **39**, 6735 (2013).
- [23] A. C. Druc, A. I. Borhan, A. Diaconu, A. R. Iordan, G. G. Nedelcu, L. Leontie, M. N. Palamaru, Ceram. Int. **40**, 13573 (2014).
- [24] A. Manikandan, L. J. Kennedy, M. Bououdina, J. J. Vijaya, J. Magn. Magn. Mater. **349**, 249 (2014).
- [25] M. A. Gabal, S. S. Ata-Allah, Chem. Phys. **85**, 104 (2004).
- [26] T. Aswani, V. Pushpa Manjari, B. Babu, Sk. Muntaz Begum, G. Rama Sundari, K. Ravindranadh, R. V. S. S. N. Ravikumar, J. Mol. Struct. **1063**, 178 (2014).
- [27] A. R. West, John Wiley & Sons, London, 1984.
- [28] K. M. Batoo, S. Kumar, C. G. Lee, Current Appl. Phy. **9**, 826 (2009).
- [29] M. Mamiya, K. Tokiwa, J. Akimoto, J. of Power Sources, **310**, 12 (2016).
- [30] E. Rezlescu, N. Rezlescu, C. Pasnicu, M. L. Craus, P. D. Popa, Crystal Research and Technology **31**, 343 (1996).
- [31] Daniela Carta, Maria Francesca Casula, Andrea Falqui, Danilo Loche, Gavin Mountjoy, Claudio Sangregorio, Anna Corrias, Journal of Physical Chemistry C **113**, 8606 (2009).